JOURNAL OF VIROLOGY, May 1997, p. 3474–3483 Vol. 71, No. 5
0022-538X/97/$04.00+0

Structure-Function Studies of the Human Immunodeficiency Virus Type 1 Matrix Protein, p17

PAULA M. CANNON,[1]† STEPHEN MATTHEWS,[2]‡ NIGEL CLARK,[1] ELAINE D. BYLES,[1] OLEG IOURIN,[1] DAVID J. HOCKLEY,[3] SUSAN M. KINGSMAN,[1] AND ALAN J. KINGSMAN[1]*

Retrovirus Molecular Biology Group, Department of Biochemistry,[1] and Department of Biochemistry and Oxford Centre for Molecular Sciences,[2] University of Oxford, Oxford OX1 3QU, and National Institute for Biological Standards and Control, South Mimms, Hertfordshire EN6 3QG,[3] United Kingdom

Received 23 September 1996/Accepted 27 January 1997

The human immunodeficiency virus type 1 (HIV-1) matrix protein, p17, plays important roles in both the early and late stages of the viral life cycle. Using our previously determined solution structure of p17, we have undertaken a rational mutagenesis program aimed at mapping structure-function relationships within the molecule. Amino acids hypothesized to be important for p17 function were mutated and examined for effect in an infectious proviral clone of HIV-1. In parallel, we analyzed by nuclear magnetic resonance spectroscopy the structure of recombinant p17 protein containing such substitutions. These analyses identified three classes of mutants that were defective in viral replication: (i) proteins containing substitutions at internal residues that grossly distorted the structure of recombinant p17 and prevented viral particle formation, (ii) mutations at putative p17 trimer interfaces that allowed correct folding of recombinant protein but produced virus that was defective in particle assembly, and (iii) substitution of basic residues in helix A that caused some relocation of virus assembly to intracellular locations and produced normally budded virions that were completely noninfectious.

The human immunodeficiency virus type 1 (HIV-1) matrix protein (MA), p17, plays a pivotal role in the virus life cycle. Situated at the amino terminus of both $p55^{gag}$ and $p160^{gag\text{-}pol}$, it directs these precursor polyproteins to the plasma membrane, where assembly and budding of viral particles occurs (15). Membrane localization requires both the cotranslational myristoylation of p17 (1, 19) and a cluster of basic amino acids at its amino terminus (44, 45). The Gag polyproteins assemble into a network of ring-like structures at the plasma membrane, producing the icosahedral structure of the viral core (33). Following proteolytic cleavage within the maturing viral particle, p17 remains in a shell directly underneath the lipid envelope of the virus, suggestive of an assembled network (16). Expression of simian immunodeficiency virus (SIV) MA alone in baculovirus systems results in the formation of virus-like particles (18), indicating that MA contains determinants of self-association.

The incorporation of the viral envelope glycoprotein, gp160, into virions is not necessary for the process of particle formation. However, the coexpression of Env proteins influences the plasma membrane site of assembly of HIV-1 Gag particles (27, 35), which suggests a specific interaction between the two proteins. The location of p17 at the membrane-proximal amino terminus of the Gag precursor and its close association with the membrane in the mature particle implicates p17 in the process of specific Env incorporation. In support of this hypothesis, p17 viral mutants whose primary defect appears to be the incorporation of gp160 into viral particles have now been identified (7, 10, 12, 41). In addition, the presence of HIV-1 MA protein in chimeric visna virus Gag cores is sufficient to recruit HIV-1 Env into the viral particles (7), and SIV Env colocalizes with SIV MA particulate material in sucrose gradients of baculovirus-derived material (18). The p17-gp160 interaction appears to involve a patch of hydrophobic residues in p17 (11) and certain structures within the cytoplasmic tail of gp41 (11, 42). Furthermore, the characteristics of this interaction show some cell type specificity, suggesting the additional involvement of cellular factors (28).

p17 is also involved in the early stages of a new infection. Certain C-terminal mutants of p17 have been shown to be defective in the ability to synthesize viral DNA following infection, suggesting a role for p17 in penetration or uncoating (43). In addition, a subset of p17 molecules have been shown to remain associated with the core-derived preintegration complex (PIC) following entry of the virus into a cell (4). The minor population of p17 molecules associated with the PIC is phosphorylated differently from the majority of the matrix protein (2, 13), a modification which has been suggested as being necessary to overcome the inherent membrane-targeting properties of myristoylated p17 and to allow the functioning of a nuclear localization signal (NLS) identified at the amino terminus of the molecule (2, 13). The mechanism whereby this population of p17 molecules is recruited into the PIC and contributes to nuclear import remains unclear, but it has been shown that phosphorylation of a C-terminal tyrosine of p17 allows an interaction with the integrase (IN) protein, which could account for the incorporation of p17 into the PIC in the producer cell (14). The presence of karyophilic p17 in the PIC provides one route whereby HIV can access the nucleus of nonmitotic cells (3), which is in contrast to observations for simpler oncoretroviruses (26) and likely contributes to the in vivo tropism of HIV. Indeed, in vitro infection of macrophages has been shown to require one of two independent routes of

* Corresponding author. Mailing address: Department of Biochemistry, University of Oxford, South Parks Road, Oxford OX1 3QU, United Kingdom. Phone: (44) 1865 275248. Fax: (44) 1865 275259.

† Present address: Gene Therapy Laboratories, Norris Cancer Centre, USC School of Medicine, Los Angeles, CA 90033.

‡ Present address: Department of Biochemistry, Imperial College of Science, Technology and Medicine, London SW7 2AY, United Kingdom.

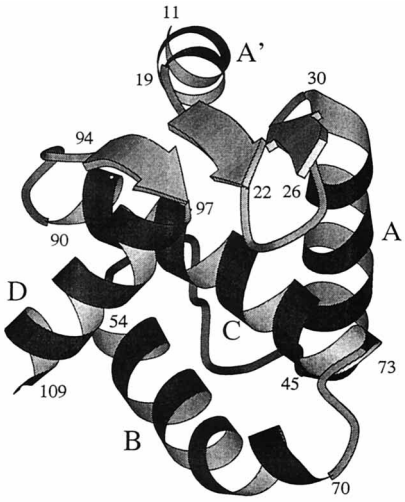

p17 AMINO ACID SEQUENCE

MGARASVLSG	GELDRWEKIR	LRPGGKKKYK	LKHIVWASRE
LERFAVNPGL	LETSEGCRQI	LGQLQPSLQT	GSEELRSLYN
TVATLYCVHQ	RIEIKDTKEA	LDKIEEEQNK	SKKKAQQAAA
DTGHSSQVSQ	NY		

FIG. 1. Refined solution NMR structure of p17. The schematic representation of HIV-1 p17 shows the relative positions of the five α helices and the β sheet and the amino acid coordinates. The diagram was produced by using MOLSCRIPT (25).

nuclear import, either through the p17 NLS or through Vpr (20, 39), although the relevance of this model been challenged (9).

We (30) and others (29) have previously determined the three-dimensional (3D) solution structure of p17 by nuclear magnetic resonance spectroscopy (NMR) (Fig. 1). Crystallographic studies have further demonstrated that the basic multimer of p17 is a trimer (21, 36). The globular central core of the protein forms a compact fold consisting of four helices, with striking structural homology to gamma interferon. In addition, the protein contains a highly basic platform consisting of three β strands. The targeting of $p55^{gag}$ to the plasma membrane requires the basic residues present on these strands (44, 45), and the NLS is also located in this region (residues 25 to 33) (3).

Previous mutational analyses of p17 have identified both single amino acids and regions of the protein that appear essential for p17 function (reviewed in reference 29). However, our structural data predict that some of these defective phenotypes could have arisen simply because of a gross distortion of the overall structure of p17, rather than as a result of the substitution of a functionally important residue. In the light of our structural model, we have now undertaken a rational mutagenesis program aimed at precisely mapping structure-function relationships within p17. Mutations of p17 were made at positions predicted to be surface exposed and therefore good candidates for involvement in the processes of particle assembly, membrane association, envelope incorporation, or PIC function. The mutations were introduced into an infectious proviral clone of HIV-1 and analyzed for their effects on the various stages of the viral life cycle. In a complementary approach, defective mutants identified in the viral assays were expressed as recombinant p17 protein, and their structures were analyzed by NMR. These approaches have now identified several classes of p17 mutants whose defects can be correlated with the various functions of the protein.

MATERIALS AND METHODS

Production of 17 mutant viruses. Single-site mutations were introduced into the proviral clone WI3 (23), using mismatched PCR primers extending from convenient restriction sites within the p17 coding sequence. All mutations were confirmed by sequencing the final reconstituted proviral DNA. Virus was generated by overnight calcium phosphate transfection of 293T cells as described previously (6). Cells were grown in Dulbecco modified Eagle medium supplemented with 10% fetal calf serum (GIBCO BRL) and transfected at 70% confluence with 30 μg of plasmid DNA per 10-cm-diameter dish. Supernatants were harvested 48 h posttransfection, clarified by centrifugation, and filtered through 0.45-μ-pore-size filters. Virus stocks were treated with DNase I (Promega) for 1 h at 37°C in the presence of 6 mM $MgCl_2$ and stored in aliquots at −70°C. Virus production was measured by p24 enzyme-linked immunosorbent assay (Coulter) or reverse transcriptase (RT) assay, using a Quant-T-RT kit (Amersham International).

Infectivity assays. Virus stocks were assayed for infectivity in the T-cell line C8166. A total of 5×10^5 cells were incubated in 1 ml of virus (approximately 500 ng of p24) for 1 h at 37°C and then washed and plated in 2 ml of fresh medium (RPMI containing 10% fetal calf serum). Infectivity was scored 2 to 3 days later by the appearance of syncytia. Virus stocks were also used to infect the H9 T-cell line. A total of 3×10^6 cells were incubated with equal amounts of wild-type and mutant viruses (as measured by RT activity) in a total volume of 1 ml for 1 h and then washed and plated in 5 ml of medium. Samples of the culture supernatant were taken every 3 to 4 days and assayed for RT activity to monitor virus production. Infectivity was also assayed using MAGI cells (24). Equivalent volumes of viral supernatants from transient transfections of 293T cells were used to infect MAGI cells plated at 20% confluence in 24-well plates. The cells were stained for β-galactosidase activity 48 h later as described previously (24), and the number of cells staining blue was determined by light microscopy. All infections were performed with at least two independently produced virus stocks for each mutant tested.

Analysis of viral proteins. Viral proteins were concentrated from the supernatants of transfected 293T cells by centrifugation through a 20% sucrose cushion at 50,000 rpm at 4°C for 2 h, using a TL100.4 rotor. The pellets were resuspended in 40 μl of loading buffer and stored at −70°C. Aliquots were heated to 90°C for 5 min before analysis by sodium dodecyl sulfate (SDS)-polyacrylamide gel electrophoresis (PAGE). HIV-1 proteins were detected by Western blotting using pooled serum from HIV-1-infected donors at 1:500 dilution. A specific anti-p17 monoclonal antibody (Capricorn, Scarborough, Maine) was used at 1:500 dilution. The secondary antibodies used were horseradish peroxidase-conjugated goat anti-human immunoglobulin and goat anti-rabbit immunoglobulin (Vector Laboratories), used at 1:1,000 and 1:4,000 dilutions, respectively. Specific interactions were visualized by using the Amersham enhanced chemiluminescence detection system.

Electron microscopy. Transfected 293T cells were fixed in 2.5% glutaraldehyde for 30 min, postfixed in 1% osmium tetroxide in isotonic buffer, and then treated with 0.5% aqueous uranyl acetate, dehydrated in ethanol, and embedded via epoxy propane in Araldite resin. Sections were cut with a diamond knife, stained with uranyl acetate and lead citrate, and examined with a Philips 210C electron microscope.

PCR analysis. One million C8166 cells were infected with equal amounts of DNase-treated virus for 1 h as described above. Total DNA was isolated from 10^6 cells 48 h postinfection, using a Qiamp genomic DNA extraction kit (Qiagen). DNA from 10^4 cell equivalents was subject to PCR, using final reaction conditions of 2 mM $MgCl_2$, 4 mM deoxynucleoside triphosphates, 1× *Taq* polymerase reaction buffer (Promega), 10 ng of each oligonucleotide primer per ml, and 0.1 U of *Taq* polymerase (Promega) per reaction. The PCR conditions were 25 cycles of 95°C for 30 s, 61°C for 30 s, and 72°C for 1 min, using primers 5′-GTCTGTTGTGTGACTCTGGT-3′ and 5′-GAGGCTTAAGCAGTGGGTTC-3′, followed by nested PCR on 1/100 of this initial reaction, using primers 5′-GTCAGTGTGGAAAATCTCTAGCA-3′ and 5′-CAGATCTGGTCTAACCAGAG-3′, for a further 25 cycles. The expected final band of 529 bp was detected by Southern blotting using a ^{32}P end-labeled oligonucleotide probe specific for the U3 region of the long terminal repeat (LTR) as described previously (5).

Recombinant protein production. p17 was expressed in *Escherichia coli* as a glutathione *S*-transferase (GST) fusion protein and purified as described previously (30). The purity of the recombinant protein was confirmed by SDS-PAGE and high-performance liquid chromatography analyses.

NMR analysis. NMR analysis was performed essentially as described previously (30). One-dimensional ^1H NMR spectra were recorded at 600 MHz and 298 K. The protein sample concentrations used were approximately 0.2 mM, and the pH was buffered at pH 6.0 with 15 mM phosphate buffer.

Peptide inhibition experiments. A series of overlapping p17-derived 15-mer peptides was obtained from the MRC AIDS Directed Program. The peptides were dissolved in phosphate-buffered saline (pH 7.0) and used at a final concen-

TABLE 1. Properties of p17 mutants

Construct[a]	Side chain[b]	Particle production			Infectivity		
		RT activity[c]	Western	Electron microscopy	C8166[d]	H9[e]	MAGI[f]
Wild type		+++	Normal	Mature, budding particles	+++	+++	100
Mutants							
Helix A							
R39E,R43E	Exposed, charged	+++	Normal	Relocation to cytoplasm	+	−	0.3
A-B loop							
F44H	Exposed, hydrophobic	+++	Normal	ND	+++	+++	ND[j]
A45I	Exposed, hydrophobic	+++	Normal	Mature, budding particles	+	+	7
V46E	Exposed, hydrophobic	+++	Normal	Mature, budding particles	+	++	44
N47D,E55Q	Exposed, charged	+++	Normal		+++	+++	ND
L50A,L51A	Internal	+	Low protein[i]	No particles	−	−	0
Helix B							
C57S	Internal	+	Low protein	No particles	−	−	0.2
Q59E	Exposed, charged	+++	Normal	ND	+++	+++	ND
Q63E	Exposed, charged	+++	Normal	ND	+++	+++	ND
B-C loop							
T70A,S72A	Exposed, hydrophilic	+++	Normal	ND	+++	+++	60
T70E,E74K	Exposed, hydrophilic	+	Low protein	No particles	+	−	0.9
Helix C							
Y86R	Internal	+++	Normal	ND	+++	+++	70
C87S	Internal	+++	Normal	Some normal particles	+	+++	5
Y86R,C87S	Internal	+	Low protein	ND	−	−	ND
Helix D							
E107K,K110E	Exposed, charged	+++	Normal	ND	+++	+++	ND
K(110-114)Q[g]	Exposed, charged	+++	Normal	ND	+++	++	ND
K(110-114)E	Exposed, charged	+++	Normal	ND	+++	+++	ND

[a] Mutants named according to amino acid substitution.
[b] Position and characteristics of the side chain of the wild-type residue.
[c] +++, wild-type activity; +, less than 20% of wild-type activity.
[d] Syncytia scored 48 h postinfection. +++, wild-type level; +, few syncytia.
[e] Time to peak RT activity in H9 cells. +++, wild-type level; ++, delayed by 2 to 5 days; +, delayed by more than 20 days.
[f] Number of blue cells per field of view relative to the wild type.
[g] Mutant is K110Q, K112Q, K113Q, K114Q.
[h] Reduced levels of viral proteins seen on Western blots.
[i] Normal profile but mobility of p17 altered.
[j] ND, not determined.

tration of 200 μg/ml. For each peptide, 2×10^5 U937 cells were pelleted and resuspended in 500 μl of medium containing 50 μl of a stock of HIV-1_{IIIB} (giving a multiplicity of infection of 0.25) and 200 μg of the appropriate peptide per ml. Following incubation for 2 days, the cells were pelleted and resuspended in fresh medium containing peptide. After a further 3 days of incubation, 100 μl of the culture was removed and added to 10^5 C8166 cells in a total volume of 500 μl with the appropriate peptide. Samples of both the U937 and C8166 culture supernatants were taken after a further 2 and 3 days of incubation and assayed for RT activity. In addition, the C8166 cells were visually inspected for the appearance of syncytia on day 3.

RESULTS

Rational mutagenesis of p17. We have previously determined the solution structure of p17 by NMR (30). A refined version of the structure, which contains an additional small helix at the amino terminus, is shown in Fig. 1 (31). On the basis of this structure, we have chosen to mutate the amino acids shown in Table 1. Our rationale was to mutate residues that are exposed on the surface of the protein and are therefore more likely to be involved in protein-protein interactions. This approach will also reduce the likelihood of interfering with the global structure of the protein. Recent crystallographic data have identified residues that are involved in p17-p17 interactions within a trimer (21, 36), and we have mutated several of these residues. In addition, we also chose to analyze mutations at positions C57 and C87, as these residues have previously been shown to be required for p17 function in other studies (12, 17, 32).

Virus production by p17 mutants. p17 mutants were introduced into an infectious proviral clone WI3 (a *nef*+ version of HXB2). The mutants were analyzed for the ability to produce virus particles following transient transfection of 293T cells by measuring RT activity in the supernatant and by Western blot analysis (Table 1 and Fig. 2). Several of the mutations clearly caused a defect in particle production, giving rise to low RT titers in the supernatant and low amounts of viral proteins on Western blots. This group of mutants included the single substitution C57S and the double substitutions L50A,L51A, Y86R,C87S, and T70E,E74K. An analysis of lysates of the transfected cells by Western blotting revealed wild-type levels of viral proteins (Fig. 2 and data not shown), suggesting that the defect in particle production occurred at assembly or release. In addition, examination of electron micrographs of the transfected cells failed to detect any particles for mutant C57S, L50A,L51A, or T70E,E74K (data not shown).

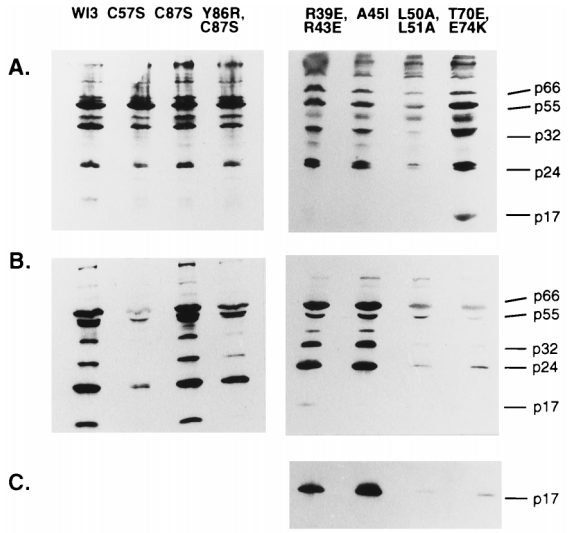

FIG. 2. Western blot analysis of p17 mutant viruses. Extracts of transfected cells (A) or virus concentrated from the supernatant (B and C) were separated on an SDS–12.5% polyacrylamide gel and probed with HIV-positive patient serum (A and B) or an anti-p17 monoclonal antibody (C). The positions of the major viral proteins, p66 (RT), p55 (Gag), p32 (IN), p24 (CA), and p17 (MA), are indicated. Mutations C57S, Y86R,C87S, L50A,L51A, and T70E,E74K all resulted in little viral material in the supernatant relative to cell extracts compared to the wild-type virus WI3. The p17 protein from mutants R39E,R43E and A45I was not recognized by HIV-positive patient serum but was revealed by an anti-p17 monoclonal antibody (C).

Infectivity of p17 mutant viruses. The infectivity of each of the various p17 mutants was compared to that of the parental wild-type virus WI3 in two T-cell lines, C8166 and H9. C8166 cells are highly sensitive to the cytopathic effects of HIV-1, and a productive infection results in visible syncytia at 24 to 72 h postinfection. H9 cells are less susceptible to killing by HIV-1, and the kinetics of a spreading infection can be monitored in these cells over a period of several days by measuring supernatant RT activity.

The majority of the mutant viruses examined [F44H, N47D, E55Q, Q59E, Q63E, T70A,S72A, Y86R, R91E, E107K,K110E, K(110-114)Q, and K(110-114)E] displayed wild-type levels of infectivity in both T-cell lines (Table 1). In agreement with this wild-type infectivity profile, none of these substitutions perturbed viral particle production as assessed by RT or Western analysis. In contrast, the group of mutants that displayed severe defects in particle production not surprisingly revealed complete (C57S, L50A,L51A, Y86R,C87S) or substantial (T70E, E74K) reductions in viral infectivity. In addition, we identified a third class of mutants which, although appearing to have no defect in viral particle production, displayed delayed replication kinetics in H9 cells. These partially defective mutants were the substitutions A45I, V46E, and C87S. In addition, mutant R39E,R43E, while not affecting particle production, resulted in a complete loss of infectivity in H9 cells and produced only a small amount of syncytia in the C8166 assay.

The infectivity of the mutant viruses was also measured in the MAGI indicator cell line (24). A successful HIV-1 infection leads to the induction of β-galactosidase activity from an integrated LTR-LacZ reporter construct, allowing measurement of the infectious titer of the viral stock. A good agreement was observed between the results of the MAGI assay and the infectivity data obtained from the T-cell lines. p17 mutants with delayed replication kinetics in H9 cells (A45I, V46E, and C87S) gave between 5 and 44% of the wild-type level of titer in the MAGI assay, correlating somewhat with the severity of the defect in H9 replication kinetics. The mutants with a more severe phenotype (R39E,R43E, L50A,L51A, C57S, and T70E, E74K) produced less than 1% of the wild-type titer.

Virion morphology and membrane localization of defective mutants. The replication-defective p17 mutant viruses appeared to fall into two groups. First, mutants L50A,L51A, C57S, and Y86R,C87S resulted in low supernatant RT levels, produced low quantities of virion-associated proteins, and demonstrated no infectivity in any of the assay systems used. Similarly, mutant T70E,E74K had reduced levels of RT and viral particles in the supernatant of transfected cells and displayed only a very slight infectivity on C8166 cells. However, a second group of mutants, which included R39E,R43E, A45I, V46E, and C87S, were partially or fully defective in the infectivity assays, despite producing wild-type levels of supernatant RT activity and having virion protein compositions that appeared normal.

The defective p17 mutant viruses were examined by electron microscopy. In agreement with the other assays for viral particle production, no virions were detected for mutant L50A, L51A, C75S, or T70E,E74K. However, mature budding particles were seen at the plasma membrane of mutants A45I, V46E, and C87S. Within the limits of resolution of this type of analysis, all of these mutants appeared to produce normal mature virions, although there was a greater tendency to see immature particles with mutant V46E (data not shown). Mutant R39E,R43E showed both mature particles budding from the plasma membrane and some relocation of viral budding away from the plasma membrane and toward intracellular vacuoles (Fig. 3B).

Envelope incorporation into defective p17 mutants. For the group of p17 mutants that produced normal levels of viral particles yet were defective in replication, the defect could be the result of inefficient incorporation of the envelope protein gp160 into budding viral cores. Previous mutational analyses of p17 have identified mutants with such phenotypes (7, 10, 41). We therefore examined the ratio of Gag (p17) to envelope (gp41) proteins present in virions purified through a 20% sucrose cushion (Fig. 4). Viral proteins were detected with both HIV-positive patient sera and monoclonal antibodies directed against p17 and gp41. Some of the substitutions introduced between residues 39 and 46 disrupted the major p17 epitope recognized by the patient sera (Fig. 4A), as has previously been reported for a Δ41-43 mutant (7). However, these mutants were recognized efficiently by the anti-p17 monoclonal antibody (Fig. 4B), indicating that these substitutions did not affect p17 incorporation into particles. Examination of the Western blots revealed that all of this group of p17 mutants had p17/gp41 ratios similar to that of the wild type, suggesting that the defect in infectivity was not caused by a lack of envelope incorporation. In addition, no defect was seen in the amount of gp120 detected in particles (data not shown).

Two-LTR circles in cycling T cells. Two-LTR circles are a form of viral DNA found only in the nucleus of cells. They therefore represent a useful marker for successful reverse transcription and nuclear import (3). We analyzed the formation of two-LTR circles by nested PCR amplification for the wild-type virus and the severely defective p17 mutants R39E,R43E, A45I, C57S, L50A,L51A, and T70E,E74K (Fig. 5). Mutants C57S and L50A,L51A, which had previously demonstrated no infectivity in any of the assays used, gave no signal. However, mutants R39E,R43E and T70E,E74K produced a band of the expected size. Both of these two mutants had previously been shown to produce a small of amount of syncytia in C8166 infections, suggesting a low level of infectivity.

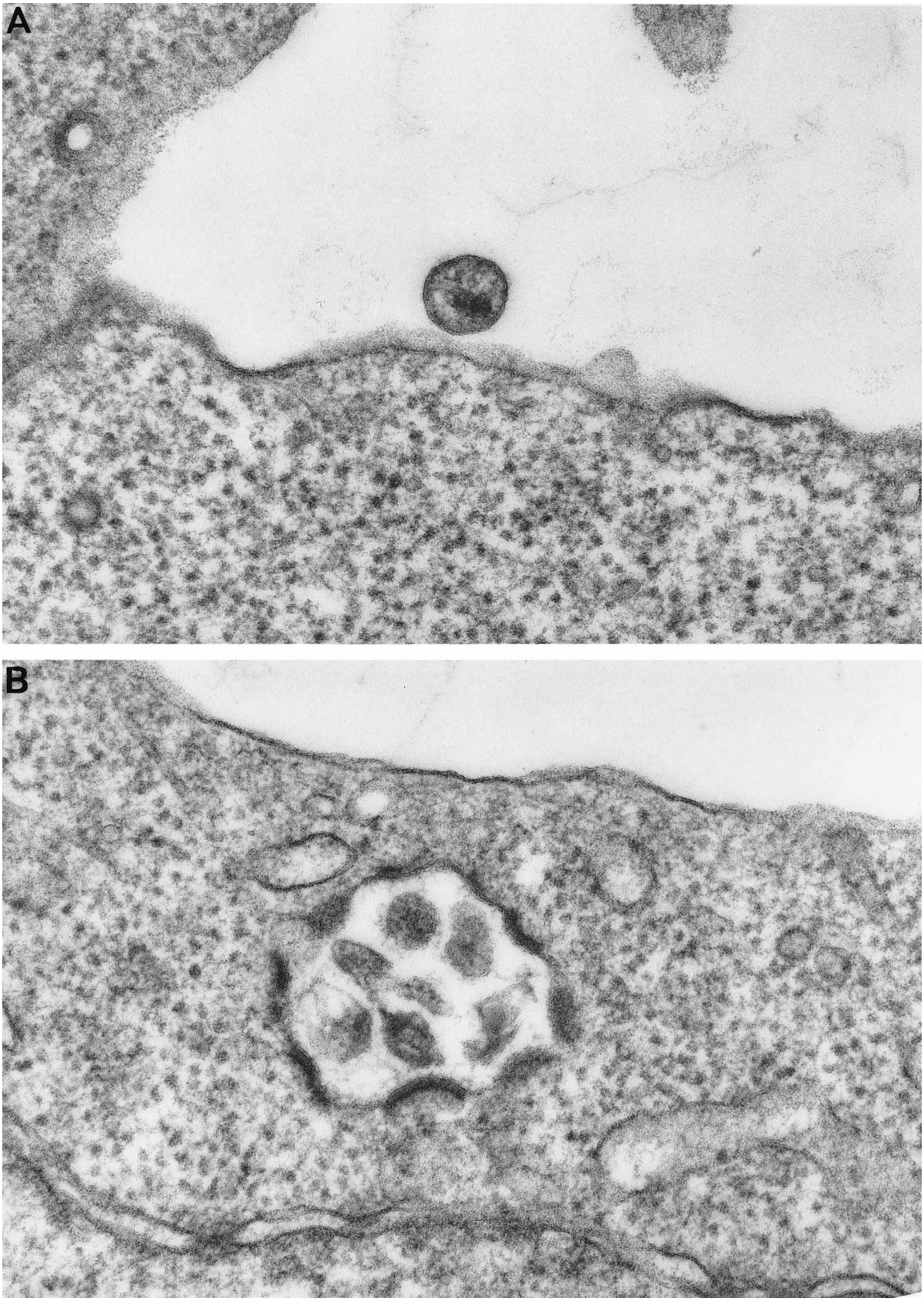

FIG. 3. Electron microscopy. (A) Wild-type virus; (B) R39E,R43E mutant virus. Mutant R39E,R43E shows some relocalization away from the plasma membrane toward internal membranes.

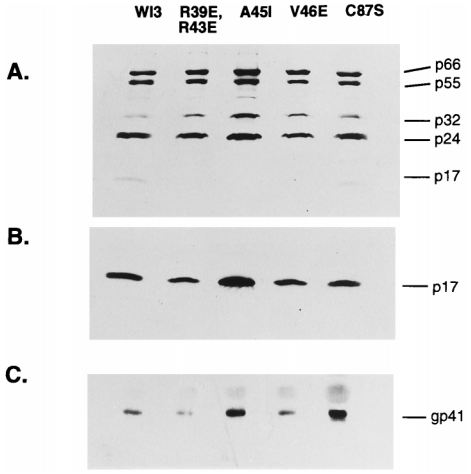

FIG. 4. Envelope incorporation into defective p17 mutant viruses. Viral proteins in the supernatants of transfected cells were pelleted through a 20% sucrose cushion and analyzed by SDS-PAGE and Western blotting. Blots were probed with HIV-positive patient sera (A) or anti-p17 monoclonal antibody (B). The membranes from panel B were then stripped and reprobed with an anti-gp41 monoclonal antibody (C).

Biophysical characterization of defective p17 mutants. The mutant p17 proteins that had been identified as affecting viral infectivity were expressed as GST fusion proteins in *E. coli* and purified as described previously (30). Mutants R39E,R43E, A45I, V46E, C87S, and T70E,E74K were readily purified by our standard procedure. However, the mutants C57S and L50A,L51A were difficult to purify, with a much greater tendency to aggregate than the wild-type protein. A small amount of purified C57S p17 was obtained, but its analysis by both circular dichroism and NMR revealed that the protein was completely unfolded (data not shown). It seems highly likely, therefore, that mutation of this central residue had grossly distorted the global structure of p17.

Amino acid C87 is also a partially buried residue. Recombinant protein containing the C87S substitution was purified by the same protocol as used for the wild-type protein, and its NMR spectrum was analyzed. The data showed it to adopt the same global fold as wild-type p17, although there were some small changes in chemical shift (<0.2 ppm) of the high-field methyl group resonances (data not shown). These well-resolved resonances were shifted upfield as a result of ring currents from at least one neighboring aromatic residue, indicating changes in the local 3D structure. Although unambiguous assignments are not possible at this stage, some small structural consequences were apparent. The high-field methyl groups resonances that show altered chemical shifts (L61, L65, and L85) share one structural feature, being part of the interface between the two helices of the coiled coil (helices B and C), whereas the mutated residue C87 lies at one end. This seems to indicate that the cavity created by a conservative cysteine-to-serine substitution resulted in a small movement (<0.5 Å) of the coiled coil.

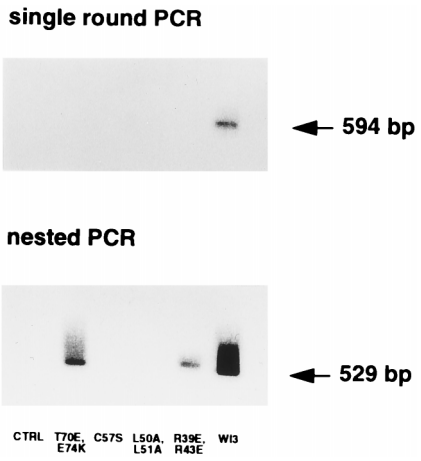

FIG. 5. Two-LTR circles. Extracts from C8166 cells infected 48 h previously with wild-type or mutant virus were subjected to single-round (A) and nested (B) PCR with primers specific for two-LTR circle junctions. The PCR products were separated on an agarose gel, and specific bands were detected by hybridization with a ^{32}P-labeled oligonucleotide probe. CTRL, uninfected C8166 cells.

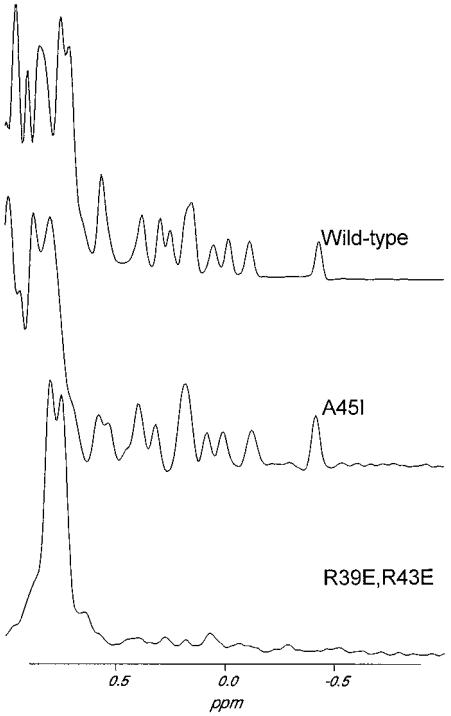

FIG. 6. NMR spectra. The methyl group region from the proton NMR spectra of wild-type p17 and mutants A45I and R39E,R43E are shown. The well-dispersed methyl signals of wild-type p17 and A45I indicate a highly structured protein, and the similarity of the two spectra implies identical structures. The lack of significant amounts of well-resolved resonances for R39E,R43E is indicative of random coil configuration.

Recombinant protein was also readily obtained for the defective p17 mutants A45I, V46E, and T70E,E74K. All three of these mutants contain substitutions at residues predicted to be located on the outside of the protein at the trimer interface (21, 36). They each produced NMR spectra essentially identical to that of wild-type p17 (Fig. 6 and data not shown), indicating that they have the same structure as the wild-type molecule, with no significant rearrangements. The lack of infectivity of the viral particles containing these mutants therefore probably reflects a defect in p17-p17 interactions within the basic trimeric unit. Mutant R39E,R43E was also purified as recombinant protein and examined by NMR. The majority of this protein was unfolded, although a fraction did appear to have the wild-type fold.

p17 peptides inhibit virus replication. It has previously been reported that the addition of a short peptide corresponding to

TABLE 2. Inhibition of HIV-1 infectivity by p17-derived peptides

Peptide[a]	RT titer (10^3 cpm/ml)[b]				Syncytia in C8166 cells on day 3
	U937		C8166		
	Day 7	Day 8	Day 2	Day 3	
None	3.2	6.7	3.9	11.4	+
31-45					−
41-55					−
51-65	14.8	47.0	19.9	33.6	+
61-75	2.1	5.7	15.4	21.9	+
71-85		1.1	3.9	3.6	+

[a] Corresponding p17 residues.
[b] RT activity in supernatant at indicated time points following challenge with HIV-1.

residues 47 to 59 of p17 can abolish HIV-1 infectivity (34). The appearance of immature and malformed virions suggested that the peptides exerted their effects at a late stage in viral assembly. We obtained a series of overlapping p17-derived peptides spanning residues 31 to 85 and examined their abilities to inhibit an acute HIV-1 infection in U937 cells. The degree of inhibition was assessed by measuring RT activity in the supernatant of the peptide-treated cultures at 7 and 8 days postinfection (Table 2). In addition, at day 5 postinfection, aliquots of the HIV-1-infected U937 cells were added to peptide-treated C8166 cells at a ratio of 1:3. Any subsequent viral spread in the more sensitive C8166 population was assessed 2 and 3 days later by measuring supernatant RT activity and by examining the cells for the appearance of syncytia.

Of the five peptides examined, two inhibited HIV-1 replication: peptide 4 (residues 31 to 45), which corresponds almost exactly to helix A; and peptide 5 (residues 41 to 55), which contains the region between helices A and B (Table 2). Peptide 5 is contained within the inhibitory peptide of residues 47 to 59 identified by Niedrig et al. (34) and likely inhibits the same process. However, it appears that we have identified a second region that can also inhibit p17 function located in helix A.

DISCUSSION

The interpretation of mutagenesis data is often hampered by an inability to distinguish between mutations that have specifically altered a functionally important residue and those that have globally affected protein structure. The determination of the 3D solution structure of the HIV-1 matrix protein p17 (29, 30) has enabled us to undertake a rational mutagenesis program aimed at mapping structure-function relationships within p17. We have specifically targeted residues that are surface exposed and therefore likely to be involved in protein-protein interactions. In addition, as crystallographic analyses of both the SIV (36) and HIV-1 (21) matrix proteins have suggested that p17 exists as a trimer, we have also introduced mutations at the putative trimer interfaces to analyze their effects on p17 function.

Mutations within the p17 coding sequence were introduced into an infectious proviral clone of HIV-1, and the effects on viral production, protein composition, virion morphology, and infectivity were analyzed. p17 mutants that resulted in viruses that were defective in one or more of these assays were then also expressed as recombinant proteins, and their structures were examined by NMR. This analysis allowed us to identify those mutations that had altered viral infectivity without adversely affecting the overall structure of the p17 molecule and to eliminate from further analyses those mutants that were defective for the more trivial reason of gross distortion of the native protein structure.

Several classes of mutants were identified. The most severe defects in viral function occurred when we made substitutions at residues predicted to be located internally. This class included the single substitution C57S as well as the double substitutions Y86R,C87S and L50A,L51A. Viruses containing these mutations were unable to form any particles at all, as shown by a lack of supernatant RT activity, low levels of viral proteins in pelleted supernatant material, and the absence of any particles in transfected cells examined by electron microscopy.

The core of p17 contains a hydrophobic pocket composed of residues V7, I34, A37, L41, L51, C57, I60, I82, and L85 (29, 30). Substitution of any of these residues could affect essential hydrophobic core interactions and prevent correct folding of the protein. When we tried to express the C57S mutation as a recombinant GST-p17 fusion protein, the protein was difficult to purify and clearly had different properties from the wild-type fusion protein. Both circular dichroism and NMR analyses of the limited amount of material that we obtained showed it to be unfolded. A GST-p17 fusion protein containing the L50A,L51A double substitution was similarly difficult to purify, with a high tendency to aggregate, and we could not produce enough material to analyze. The changes in the biochemical properties of this mutant protein probably also arise from a large distortion of the structure of p17.

We conclude therefore that this class of mutants probably interrupts the folding pathway of p17, leading to downstream effects on the Gag-Gag interactions required for viral particle assembly. Previous analyses have also reported defects in virion production for C57S substitutions (12) and an insertion between residues 57 and 58 (40). These data also provide an explanation for the gross defects in particle assembly previously reported for C57S substitutions in $p55^{gag}$ baculovirus expression systems (17, 32) and suggest that C57S is not a determinant of particle assembly *per se* but rather an important internal structural residue for p17.

While the double substitution Y86R,C87S was also defective in viral particle production, the single substitutions were either wild type (Y86R) or only partially affected (C87S). For Y86, the tyrosine ring sits in a hydrophobic pocket, making contacts with residues R58, L61, C87, Q90, and I104, with the tyrosine hydroxy solvent exposed. The C87 side chain also sits in a hydrophobic pocket, defined by residues V84, Y86, I92, V94, A100, and K103. Presumably, the substitution of a more hydrophilic residue in the C87S mutant destabilized this region, producing the slight shifts in the structure observed in the NMR spectra for the recombinant protein. Virus containing this mutation was less infectious than the wild type, in agreement with previous studies (12), but produced normal levels of viral particles. We did not observe the relocalization of particle assembly to intracellular membranes that has been reported (12), although this discrepancy could be a result of the different HIV-1 strains used in the two studies. The more severe phenotype of the double mutant Y86R,C87S presumably arises from the cumulative effects of these two neighboring substitutions.

A second group of mutants that we analyzed contained substitutions at residues predicted to lie at the interfaces between the trimers of p17 seen in crystallographic analyses (Fig. 7A) (21, 36). This group produced mutants that were less severe (V46E), intermediate (A45I), or very severe (T70E,E74K) in their phenotypes. Recombinant proteins containing these substitutions each produced NMR spectra essentially identical to that of wild-type p17, indicating that they have the same struc-

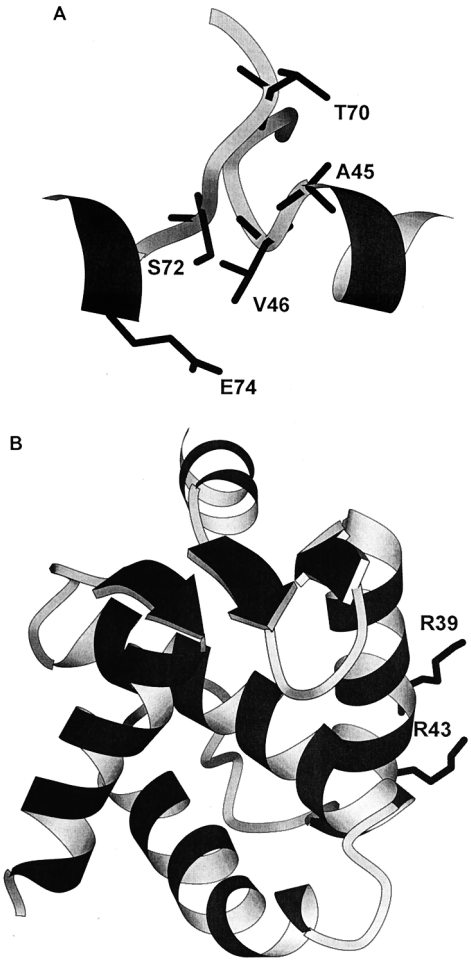

FIG. 7. (A) Schematic representation of the backbone resides of the trimer interface region (residues 41 to 49) of one monomer and residues 69 to 76 of the adjacent monomer). The trimer interface coordinates were obtained by modeling the p17 NMR structure on the SIV trimer crystal structure (36). (B) Positions of side chains of residues R39 and R43 on the outside of helix A.

ture as the wild-type molecule, with no significant rearrangements. It is therefore highly likely that the effects on viral infectivity observed for these mutants reflect a defect in p17-p17 interactions across the putative trimer interfaces.

The most extreme trimer interface mutant was the T70E, E74K double substitution, which completely prevented viral particle formation. Examination of the crystal structure of the p17 trimer suggests that there would be no room across the interface for the substitution of a larger side chain (glutamic acid) at position 70 and that the negative charge at the end of the side chain might also interact unfavorably with the neighboring molecule. The T70E,E74K mutant is therefore distinct from the previous group of mutations that also abolished particle formation, as it allowed the correct folding of the protein but was presumably defective in the p17-p17 interactions necessary for Gag assembly. Other mutations predicted to lie at the trimer interface, such as N47D,E55Q and T70A,S72A, had no effect on particle production or infectivity. The relative tolerance of these residues to change probably reflects the fact that the interactions in the trimer are backbone, not side chain, interactions (21, 36), which will allow some degree of sequence flexibility in this area.

The intermolecular interactions between p17 monomers present in the crystal structure are relatively weak and are not seen in solution. Such weak interactions may, however, be sufficient to stabilize p17-p17 interactions in the context of the larger Gag polyprotein, and SIV MA has been shown to be capable of self-assembly into viral-like particles in a baculovirus system (18). The recruitment of p17 monomers into a higher-order assembly within particles, or additional interactions with cytoskeletal components, could stabilize p17-p17 interactions even after cleavage from the Gag polyprotein during core maturation. Overall, our mutagenesis data are supportive of a model where the basic multimer of p17 is likely a trimer.

Two p17 mutants, A45I and R39E,R43E, appeared to be defective in stages of the HIV life cycle downstream of particle assembly. Several Gag mutations that also have no effect on particle assembly but abolish infectivity have previously been described (37, 40), highlighting the fact that the viral core proteins are also required for later stages in the viral life cycle. The substitution A45I resulted in normal levels of particle production, but the virus produced was almost completely noninfectious. We had predicted that the presence of the larger isoleucine side chain at the putative trimer interface would cause steric problems between residue 45 and the amino acids F44 and L75 on adjacent molecules, but viral particle production did not appear to be affected in these mutants. The presence of a higher proportion of immature particles in electron micrographs of the A45I viruses relative to the wild type may, however, indicate a defect in assembly and maturation. It is also possible that the A45I substitution interferes with postentry processes that require the disassociation of p17-p17 multimers or, alternatively, interferes with the association of the subset of p17 molecules that are part of the PIC.

A particularly interesting mutant was the R39E,R43E double substitution. These arginine residues lie on the outside of helix A (Fig. 7B) and may well be part of the basic region that is involved in localization to the plasma membrane (21). Indeed, electron microscopy analysis revealed some redirection of viral budding away from the plasma membrane toward intracellular vacuoles in this mutant. The redirection of particle assembly to intracellular membranes has also been reported for other point mutations (12) and larger deletions (8, 27) of p17. The R39E,R43E mutant did, however, produce large amounts of normally budded virions, giving rise to wild-type levels of RT activity in the supernatant of transfected cells. The virions were, however, almost completely noninfectious, producing very low levels of syncytia in C8166 cells and a low titer on MAGI cells. The virions appeared to have normal profiles by Western analysis and incorporated the envelope protein. In addition, two-LTR circles could be detected at low levels in cycling T cells, and although this was not a quantitative assay, it does imply that there is no absolute block to reverse transcription or nuclear import in these cells. Previous mutational analysis of R43 (substitution to alanine) resulted in a virus that replicated with wild-type kinetics (12). However, a linker insertion between residues 40 and 41 resulted in virions that had near-wild-type levels of particle production, incorporated envelope, but resulted in completely noninfectious virions (37). It seems likely therefore that this region plays an additional, as yet unidentified role in viral infectivity.

Incubation of HIV-1 with peptides derived from p17 identified two regions that act as inhibitors of viral replication. One inhibitory peptide corresponded to residues 41 to 55, which covers one of the predicted trimer interfaces. This peptide also contains residues 47 to 59, which were previously shown by Niedrig et al. (34) to block the formation of mature virus particles. We additionally identified a second inhibitory pep-

tide, covering residues 31 to 45. This region contains the whole of helix A, and it is tempting to speculate that the inhibitory effects of this peptide result from inhibition of the same process that is defective in the R39E,R43E mutant. Previous analysis using a larger peptide of residues 23 to 46 (34) did not inhibit HIV-1 replication. However, this larger peptide may not adopt the same structure as our shorter peptide, or the eight extra residues at the amino terminus may obscure the inhibitory domain contained within residues 31 to 45.

The least disruptive mutations that we made were in helix D. Even the change of charge from four basic to acidic residues in K(110-114)E produced a virus with a wild-type phenotype. This region is predicted to extend down from the core of the p17 molecule and possibly serves as a spacer between p17 and the CA protein, p24 (21). Other studies have also found that this region is insensitive to amino acid changes (7, 12), although a deletion of 13 amino acids (residues 116 to 128) resulted in a virus that was defective in the early postbinding stages of the viral life cycle (43).

In summary, mutations of residues in p17 had various effects on viral replication. The most disruptive substitutions that abolished particle production also prevented the correct folding of recombinant p17 fusion proteins, suggesting that the viral phenotype resulted from a gross distortion of p17 structure. Particle production was also inhibited by some mutations at the trimer interface predicted from crystallographic analysis of HIV-1 and SIV matrix proteins, supporting the idea that the trimer may be a functional intermediate in the process of particle assembly. We identified an additional group of mutants that were defective at postbudding stages of the life cycle, including A45I and the helix A mutant R39E,R43E. We also identified inhibitory peptides that spanned either a putative p17 trimer interface or corresponded to helix A.

ACKNOWLEDGMENTS

We gratefully acknowledge the generous disclosure of unpublished data by Wesley Sundquist and Christopher Hill and their insightful comments on this work.

This project was supported by grant G9230555 from the Medical Research Council AIDS Directed Program.

REFERENCES

1. **Bryant, M., and L. Ratner.** 1990. Myristoylation-dependent replication and assembly of human immunodeficiency virus 1. Proc. Natl. Acad. Sci. USA **87:**523–527.
2. **Bukrinskaya, A. G., A. Ghorpade, N. K. Heinzinger, T. E. Smithgall, R. E. Lewis, and M. Stevenson.** 1996. Phosphorylation-dependent human immunodeficiency virus type 1 infection and nuclear targeting of viral DNA. Proc. Natl. Acad. Sci. USA **93:**367–371.
3. **Bukrinsky, M. I., S. Haggerty, M. P. Dempsey, N. Sharova, A. Adzhubel, L. Spitz, P. Lewis, D. Goldfarb, M. Emerman, and M. Stevenson.** 1993. A nuclear localization signal within HIV-1 matrix protein that governs infection of non-dividing cells. Nature **365:**666–669.
4. **Bukrinsky, M. I., N. Sharova, T. L. McDonald, T. Pushkarskaya, W. G. Tarpley, and M. Stevenson.** 1993. Association of integrase, matrix, and reverse transcriptase antigens of human immunodeficiency virus type 1 with viral nucleic acids following acute infection. Proc. Natl. Acad. Sci. USA **90:** 6125–6129.
5. **Cannon, P. M., E. D. Byles, S. M. Kingsman, and A. J. Kingsman.** 1996. Conserved sequences in the carboxyl terminus of integrase that are essential for human immunodeficiency virus type 1 replication. J. Virol. **70:**651–657.
6. **Cannon, P. M., W. Wilson, E. Byles, Susan M. Kingsman, and Alan J. Kingsman.** 1994. Human immunodeficiency virus type 1 integrase: effect on viral replication of mutations at highly conserved residues. J. Virol. **68:**4768–4775.
7. **Dorfman, T., F. Mammano, W. A. Haseltine, and H. G. Gottlinger.** 1994. Role of the matrix protein in virion association of the human immunodeficiency virus type 1 envelope glycoprotein. J. Virol. **68:**1689–1696.
8. **Facke, M., A. Janetzko, R. L. Shoeman, and H.-G. Krausslich.** 1993. A large deletion in the matrix domain of the human immunodeficiency virus *gag* gene redirects virus particle assembly from the plasma membrane to the endoplasmic reticulum. J. Virol. **67:**4972–4980.
9. **Freed, E. O., G. Englund, and M. A. Martin.** 1995. Role of the basic domain of human immunodeficiency virus type 1 matrix protein in macrophage infection. J. Virol. **69:**3949–3954.
10. **Freed, E. O., and M. A. Martin.** 1995. Virion incorporation of envelope glycoproteins with long but not short cytoplasmic tails is blocked by specific, single amino acid substitutions in the human immunodeficiency virus type 1 matrix. J. Virol. **69:**1984–1989.
11. **Freed, E. O., and M. A. Martin.** 1996. Domains of the human immunodeficiency virus type 1 matrix and gp41 cytoplasmic tail required for envelope incorporation into virions. J. Virol. **70:**341–351.
12. **Freed, E. O., J. M. Orenstein, A. J. Buckler-White, and M. A. Martin.** 1994. Single amino acid changes in the human immunodeficiency virus type 1 matrix protein block virus particle production. J. Virol. **68:**5311–5320.
13. **Gallay, P., S. Swingler, C. Aitken, and D. Trono.** 1995. HIV-1 infection of non-dividing cells: C-terminal phosphorylation of the viral matrix protein is a key regulator. Cell **80:**379–388.
14. **Gallay, P., S. Swingler, J. Song, F. Bushman, and D. Trono.** 1995. HIV nuclear import is governed by the phosphotyrosine-mediated binding of matrix to the core domain of integrase. Cell **83:**569–576.
15. **Gelderblom, H. R.** 1991. Assembly and morphogenesis of HIV: potential effect of structure on viral function. AIDS **5:**617–638.
16. **Gelderblom, H. R., E. H. S. Haausmann, M. Ozel, G. Pauli, and M. A. Koch.** 1987. Fine structure of human immunodeficiency virus (HIV) and immunolocalisation of structural proteins. Virology **156:**171–176.
17. **Gonzales, S. A., and J. L. Affranchino.** 1995. Mutational analysis of the conserved cysteine residues in the simian immunodeficiency virus matrix protein. Virology **210:**501–507.
18. **Gonzales, S. A., J. L. Affranchino, H. R. Gelderblom, and A. Burny.** 1993. Assembly of matrix protein of simian immunodeficiency virus into virus-like particles. Virology **194:**548–556.
19. **Gottlinger, H. G., J. G. Sodroski, and W. A. Haseltine.** 1989. Role of capsid precursor processing and myristoylation in morphogenesis and infectivity of human immunodeficiency virus type 1. Proc. Natl. Acad. Sci. USA **86:**5781–5785.
20. **Heinzinger, N. K., M. I. Bukrinsky, S. A. Haggerty, A. M. Ragland, V. Kewalramani, M.-A. Lee, H. E. Gendelman, L. Ratner, M. Stevenson, and M. Emerman.** 1994. The vpr protein of human immunodeficiency virus type 1 influences nuclear localization of viral nucleic acids in non-dividing host cells. Proc. Natl. Acad. Sci. USA **91:**7311–7315.
21. **Hill, C. P., D. Worthylake, D. P. Bancroft, A. M. Christensen, and W. I. Sundquist.** 1996. Crystal structures of the trimeric HIV-1 matrix protein: implications for membrane association and assembly. Proc. Natl. Acad. Sci. USA **93:**3099–3104.
22. **Hunter, E., and R. Swanstrom.** 1990. Retrovirus envelope glycoprotein. Curr. Top. Microbiol. Immunol. **157:**187–253.
23. **Kim, S., R. Byrn, J. E. Groopman, and D. Baltimore.** 1989. Temporal aspects of DNA and RNA synthesis during human immunodeficiency virus infection: evidence for differential gene expression. J. Virol. **63:**3708–3713.
24. **Kimpton, J., and M. Emerman.** 1992. Detection of replication-competent and pseudotyped human immunodeficiency virus with a sensitive cell line on the basis of activation of an integrated β-galactosidase gene. J. Virol. **66:** 2232–2239.
25. **Kraulis, P. J.** 1991. Molscript—a program to produce both detailed and schematic plots of protein structures. J. Appl. Crystallogr. **24:**946–950.
26. **Lewis, P. M., M. Hensel, and M. Emerman.** 1992. Human immunodeficiency virus infection of cells arrested in the cell cycle. EMBO J. **11:**3053–3058.
27. **Lodge, R., H. Gottlinger, D. Gabuzda, E. A. Cohen, and G. Lemay.** 1994. The intracytoplasmic domain of gp41 mediates polarized budding of human immunodeficiency virus type 1 in MDCK cells. J. Virol. **68:**4857–4861.
28. **Mammano, F., E. Kondo, J. Sodroski, A. Bukovsky, and H. G. Gottlinger.** 1995. Rescue of human immunodeficiency virus type 1 matrix protein mutants by envelope glycoproteins with short cytoplasmic domains. J. Virol. **69:** 3824–3830.
29. **Massiah, M. A., M. R. Starich, C. Paschall, M. F. Summers, A. M. Christensen, and W. I. Sundquist.** 1994. Three-dimensional structure of the human immunodeficiency virus type 1 matrix protein. J. Mol. Biol. **244:**198–223.
30. **Matthews, S., P. Barlow, J. Boyd, G. Barton, R. Russell, H. Mills, M. Cunningham, N. Meyers, N. Burns, N. Clark, S. Kingsman, A. Kingsman, and I. Campbell.** 1994. Structural similarity between the p17 matrix protein of HIV-1 and interferon-γ. Nature **370:**666–668.
31. **Matthews, S., P. N. Barlow, N. Clark, S. Kingsman, A. Kingsman, and I. Campbell.** 1995. The refined solution structure of the HIV-1 matrix protein, p17. Biochem. Soc. Trans. **23:**725–728.
32. **Morikawa, Y., T. Kishi, H. Zhang, M. V. Nermut, D. J. Hockley, and I. M. Jones.** 1995. A molecular determinant of the human immunodeficiency virus particle assembly located in matrix antigen p17. J. Virol. **69:**4519–4523.
33. **Nermut, M. V., D. J. Hockley, J. B. M. Jowett, I. A. Jones, M. Garreau, and D. Thomas.** 1994. Fullerene-like organization of HIV gag-protein shell in virus-like particles produced by recombinant baculovirus. Virology **198:**288–296.
34. **Niedrig, M., H. R. Gelderblom, G. Pauli, J. Marz, H. Bickhard, H. Wolf, and**

S. Modrow. 1994. Inhibition of infectious human immunodeficiency virus type 1 particle formation by Gag protein-derived peptides. J. Gen. Virol. **75:** 1469–1474.
35. **Owens, R. J., J. W. Dubay, E. Hunter, and R. W. Compans.** 1991. Human immunodeficiency virus envelope protein determines the site of virus release in polarised epithelial cells. Proc. Natl. Acad. Sci. USA **88:**3987–3991.
36. **Rao, Z., A. S. Belyaev, E. Fry, P. Roy, I. M. Jones, and D. I. Stuart.** 1995. Crystal structure of SIV matrix antigen and implications for viral assembly. Nature **378:**743–747.
37. **Reicin, A. S., S. Paik, R. D. Berkowitz, J. Luban, I. Lowy, and S. P. Goff.** 1995. Linker insertion mutations in the human immunodeficiency virus type 1 *gag* gene: effects on virion particle assembly, release, and infectivity. J. Virol. **69:**642–650.
38. **Spearman, P., J.-J. Wang, N. Vander Heyden, and L. Ratner.** 1994. Identification of human immunodeficiency type 1 Gag protein domains essential to membrane binding and particle assembly. J. Virol. **68:**3232–3242.
39. **Von Schwelder, U., R. S. Kornbluth, and D. Trono.** 1994. The nuclear localization signal of the matrix protein of human immunodeficiency virus type 1 allows the establishment of infection in macrophages and quiescent T lymphocytes. Proc. Natl. Acad. Sci. USA **91:**6992–6996.
40. **Wang, C.-T., and E. Barklis.** 1993. Assembly, processing and infectivity of human immunodeficiency virus type 1 Gag mutants. J. Virol. **67:**4262–4273.
41. **Yu, X., X. Yuan, Z. Matsuda, T.-H. Lee, and M. Essex.** 1992. The matrix protein of human immunodeficiency virus type 1 is required for incorporation of viral envelope protein into mature virions. J. Virol. **66:**4966–4971.
42. **Yu, X., X. Yuan, M. F. McLane, T.-H. Lee, and M. Essex.** 1993. Mutations in the cytoplasmic domain of human immunodeficiency virus type 1 transmembrane protein impair the incorporation of Env protein into mature virions. J. Virol. **67:**213–221.
43. **Yu, X., Q.-C. Yu, T.-H. Lee, and M. Essex.** 1992. The C terminus of human immunodeficiency virus type 1 matrix protein is involved in the early steps of the virus life cycle. J. Virol. **66:**5667–5670.
44. **Yuan, X., X. Yu, T.-H. Lee, and M. Essex.** 1993. Mutations in the N-terminal region of human immunodeficiency type 1 matrix protein block intracellular transport of the Gag precursor. J. Virol. **67:**6387–6394.
45. **Zhou, W., L. J. Parent, J. W. Wills, and M. D. Resh.** 1994. Identification of a membrane-binding domain within the amino-terminal region of human immunodeficiency virus type 1 Gag protein which interacts with acidic phospholipids. J. Virol. **68:**2556–2569.